

# New experimental insights into self-organization of poly(ferrocenyl-amide-siloxane)

M. CAZACU\*, C. RACLES, A. VLAD, G. CALIN<sup>a</sup>, D. TIMPU, F. IACOMI<sup>a</sup>

*"Petru Poni" Institute of Macromolecular Chemistry, Aleea Gr. Ghica Voda 41A, 700487, Iasi, Romania*

*<sup>a</sup>"Al. I. Cuza" University, Faculty of Physics, Blvd. Carol I 11, 700506, Iasi Romania*

The self-organization ability of a low molecular weight ferrocenyl-amide-siloxane copolymer was investigated in solution and film. <sup>1</sup>H NMR and dynamic light scattering (DLS) have been used to emphasize that the polymer is able to form aggregates in DMF solution. Such structures can also be found in film remained after solvent evaporation as was observed by AFM and SEM. X-ray investigation on the annealed films revealed certain crystallinity. Two types of transport phenomena delimited by the glass transition temperature, T<sub>g</sub>, were identified by electrical measurements.

(Received December 2, 2009; accepted February 18, 2010)

**Keywords:** Ferrocenyl-siloxane copolymer, Polyamide, self-assembling

## 1. Introduction

It is known that, by controlling the composition, molecular weight and architectures, copolymers can form periodic mesostructures [1]. For such aim, the amphiphile nature of the copolymer is of high importance. It is well known that, due to the extremely low polarity, polysiloxanes are incompatible with almost any organic system [2]. As a result, most of the copolymers based on siloxane and organic partners are able to self-assemble in a selective solvent. This phenomenon is common for low molecular weight surfactants and block-copolymers and occurs when the concentration exceeds a threshold known as critical micelle concentration (CMC). The insertion of metal centers (especially those of transition elements) in the co-monomer sequence has been shown to facilitate access to a diverse range of interesting and useful properties. This is a consequence of the metal electronic structure, which generally exist in a variety of oxidation states. The presence of the metal is also of particular interest from the perspective of supramolecular science due to the possibility to develop weak metal-metal bonds besides classical intermolecular interactions. These represent a supplementary tool to direct the self-assembly of the copolymer into the desired morphology [1]. The self-assembly of a series of polyferrocenylsilane-polysiloxane block copolymers has been already demonstrated [3-8].

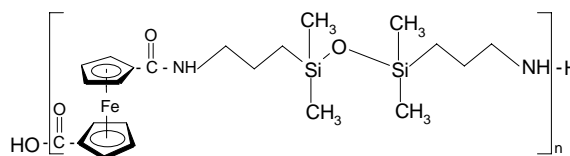
The copolymer approached in this paper, poly{1,1'-ferrocene-diamide-[1,3-bis(propylene)tetramethyldisiloxane]}, is formed by alternating disiloxane-aliphatic sequences and ferrocene units, bridged by amide groups. The siloxane-aliphatic sequence is hydrophobic, non-polar, while the ferrocenyl-diamide group is polar one. The presence within a chain of sequences having high differences in polarity constitutes a premise for the aggregation in a selective solvent. Even though the polar sequences are very short, their association in favorable thermodynamical conditions would be possible due to highly flexible siloxane bonds [9,10].

In the previous study [11], we emphasized such ability by the results of the tensiometry, viscometry and UV-Vis spectrophotometry, DLS (Microtrac Nanotracc) and SEM (BDS) studies. In the present paper, we intend to provide some additional proofs for this behavior, obtained by <sup>1</sup>H NMR and DLS (Malvern) studies in solution, as well as by AFM, and SEM (ETD) on films. The annealed films were investigated by X-ray diffraction. The electrical properties of thin films were investigated as a function of temperature.

## 2. Experimental

### 2.1 Materials

The ferrocene-siloxane polyamide CEN22 having the structure presented in Scheme 1 has been prepared as already reported in [12,13] by polycondensation of 1,1'-di(chlorocarbonyl)ferrocene with 1,3-bis(aminopropyl)tetramethyldisiloxane, in solution, at low temperature. A dark-brown solid product was obtained after separation from the reaction mixture, purification and drying. The structure was verified by spectral analysis (FTIR and <sup>1</sup>H NMR). Due to the presence in <sup>1</sup>H NMR spectra of the detectable signal for the appropriate groups ((CH<sub>3</sub>)<sub>2</sub>SiO-, (C<sub>5</sub>H<sub>4</sub>)<sub>2</sub>Fe and -NH<sub>2</sub>), an estimation of the average number molecular weight, Mn, was possible. Based on the obtained value, it can be estimated that the product is in fact an oligomer with average polycondensation degree of about 7.5.



*Scheme 1. Chemical structure of poly{1,1'-ferrocene-diamide-[1,3-bis(propylene)tetramethyl-disiloxane]}, CEN22.*

The copolymer was dissolved in DMF (0.5% solutions) and spin-coated (1000-3000 rot/min) on glass substrates. After each layer, the thin film was annealed at 100 °C for 1 min. The procedure was repeated 20 times in order to obtain thin films with a thickness around 50 nm (sample CEN22-SC). Other thin film was prepared by simple cast of the solution on glass substrate followed by a room temperature solvent evaporation (CEN22-C) and IR irradiation (300nm) for 3h (CEN22-CIR). Both film types were then slowly heated at 200°C, followed by a slow cooling (samples CEN22-SC-200, CEN22-C-200, and CEN-CIR-200). Both raw and annealed films were investigated by XRD, AFM, SEM and EDX. The electrical measurements were also performed.

## 2.2 Techniques

The  $^1\text{H-NMR}$  spectra were recorded on a BRUKER Avance DRX 400 spectrometer, using DMSO and  $\text{CDCl}_3$  as solvents. Spectra of the solutions in chloroform having different concentrations were registered at different temperatures.

Particles size and distribution were determined by dynamic light scattering (DLS) by using a Malvern Zetasizer ZS (Malvern Instruments, UK). The solution previously filtered through 0.5  $\mu\text{m}$  filter, without further dilution was irradiated with red light (HeNe laser, wavelength  $\lambda=632.8\text{nm}$ ) and the intensity fluctuations of the scattered light (detected at a back scattering angle of  $173^\circ$ ) analyzed to obtain an autocorrelation function.

Microscopic investigations were performed on an Environmental Scanning Electron Microscope (ESEM) type Quanta 200 operating at 30kV with secondary electrons detector (ETD) in high vacuum mode. Dispersive X-ray spectroscopy (EDX) coupled to the ESEM permitted to emphasize surface X-ray elemental distribution.

Atomic Force Microscopy Scanning (AFM) by SOLVER PRO-M model (NT-MDT Russia) was used to measure surfaces on a fine scale.

X-ray diffraction of the films was performed by using a BRUKER 8D diffractometer with  $\text{CuK}_\alpha$  ( $\lambda = 0.154 \text{ nm}$ ) radiation.

Electrical measurements were performed on polymer films having thickness of about 50 nm deposited on glass plates by spin coating, by using an Keithley 617 electrometer with data acquisition. The method of the two probes was applied to measure the electrical conductivity.

## 3. Results and discussion

Solutions having different concentrations were prepared based on copolymer CEN22 in different solvents ( $\text{CDCl}_3$ , DMSO- $d_6$ , and DMF) in order to be investigated by  $^1\text{H NMR}$  and DLS.

In  $^1\text{H NMR}$  spectra, the ferrocene protons peaks (4.3-4.7ppm) are better resolved in DMSO, a selective solvent for polar moiety, than in  $\text{CDCl}_3$ , which is a good solvent for the siloxane moiety (Fig. 1).

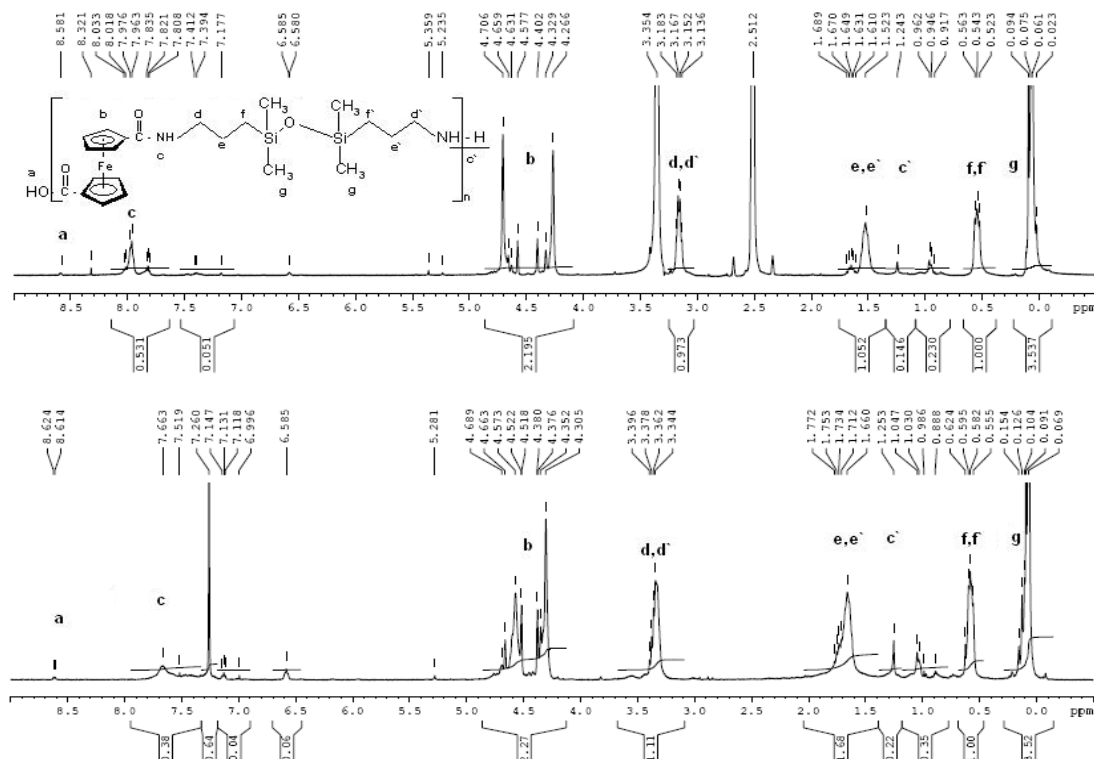


Fig. 1.  $^1\text{H NMR}$  spectra of CEN22 registered in DMSO- $d_6$  (top) and  $\text{CDCl}_3$  (down) at 25°C (0.5%w/v concentration).

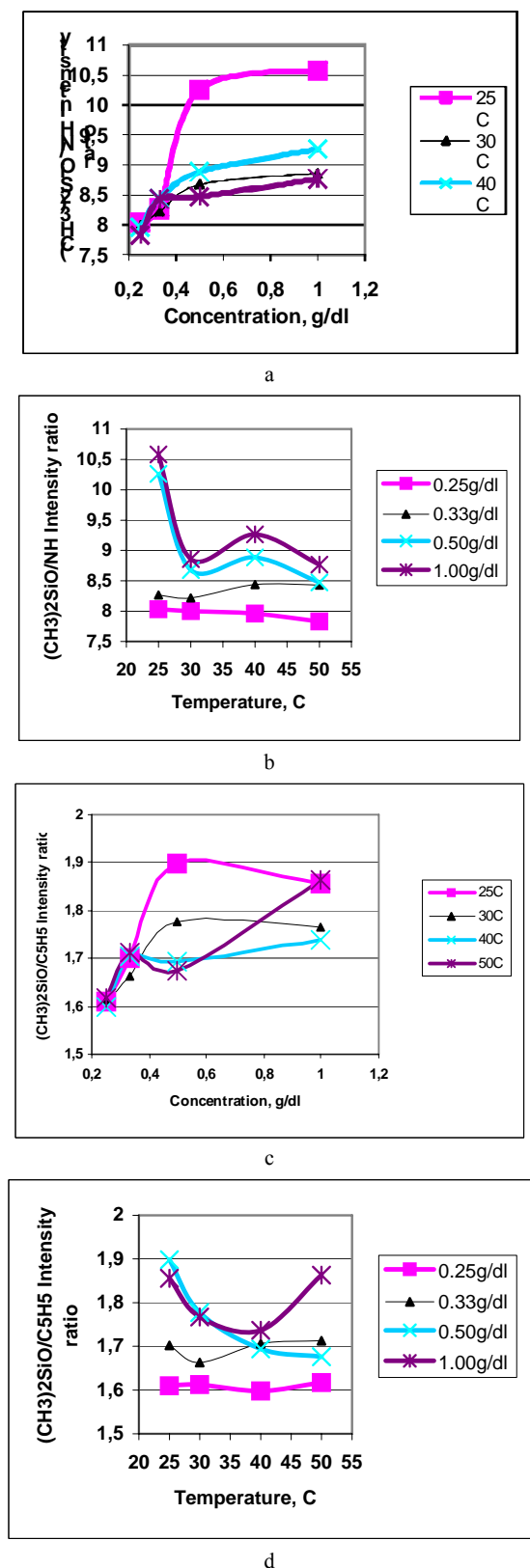


Fig. 2. Changes in the peak intensities ratios by concentration and temperature increasing for solutions in  $CDCl_3$

The explanation could be the formation of core-shell aggregates by coiling of the insoluble segment and their surrounding by soluble segment. The bad solubilization of the core segments results in a poor resolution of the corresponding peaks in  $^1H$  NMR spectra. Such a proof for the association was used in literature in the case of amphiphile copolymers [14]. In our case such aggregation could be explained by H-bonding and hydrophobic interactions. Further NMR evidences for self-assembling was obtained by registering the spectra in chloroform at different concentrations and temperatures. The modifications of the intensities ratio of the peaks assigned to the protons from polar (amide at 7.6 ppm) and nonpolar (dimethylsiloxane at 0.06-0.15 ppm) groups depending on the solution concentration and temperature are shown in Fig. 2a,b. Variations on concentration and temperature were also observed for the ratio between the peak intensities of the protons from dimethylsiloxane (0.06-0.15) and ferrocene (4.30-4.68 ppm) units (Fig. 2c,d).

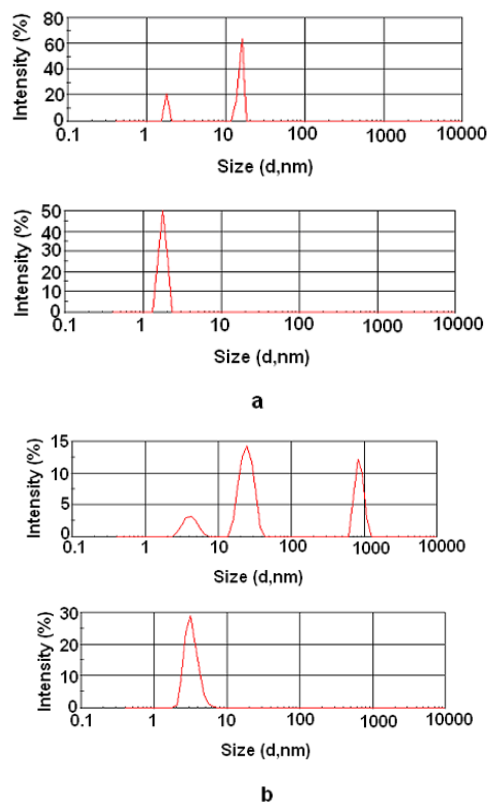


Fig. 3. The intensity (top) and volume (bottom) size distribution of the particles versus aggregates diameter in DMF solution

As can be seen, the main changes on the dependence curves occur at 0.5% and 40°C. It is very interesting that in our previous study on the same copolymer, the tensiometry, viscometry and UV-Vis absorption investigations in DMF showed the same critical concentration and temperature values [11]. Thus, we can conclude that concentration of 0.5% and the temperature of 40°C, are critical aggregation parameters in chloroform too.

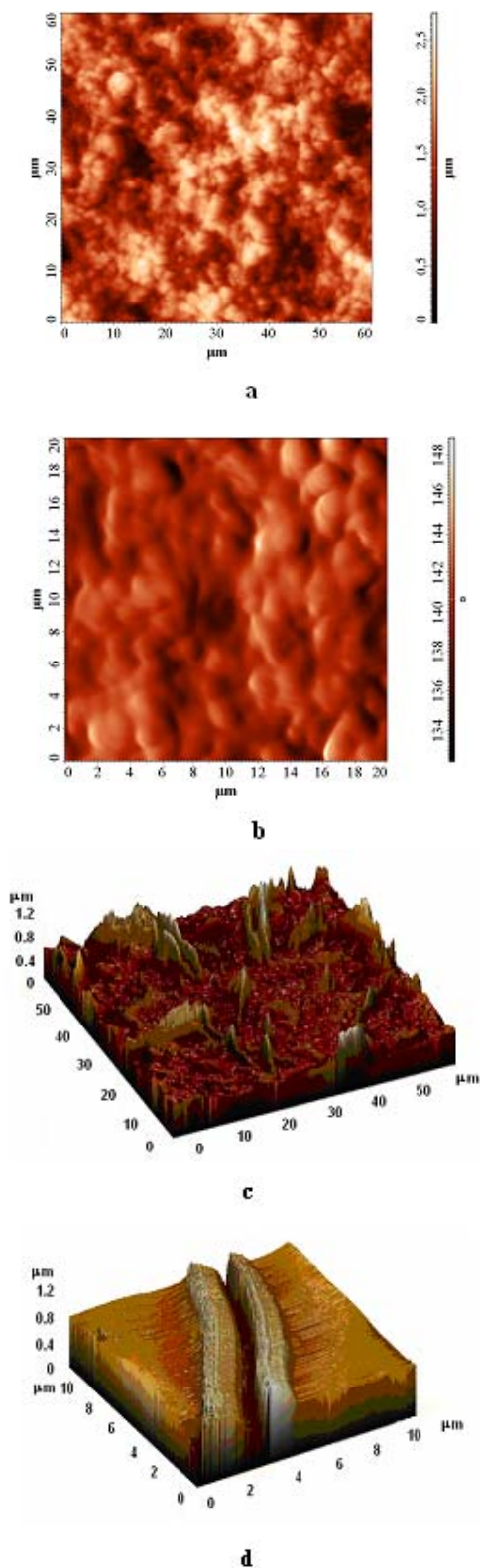


Fig. 4. AFM images of the film surface obtained by 0.5% DMF solution cast on glass substrate CEN22-C (a-2D; b-phase), CEN22-CIR-200 (c - 60x60 $\mu\text{m}$  3D, d-10x10 $\mu\text{m}$  3D).

Fig. 3a shows the intensity size distribution of the particles formed by copolymer in DMF at 0.5% w/v concentration. Two populations can be identified, one having a diameter around 2 nm and another about 20 nm that are the result of the association phenomena. However, only a population is emphasized in the volume size distribution, namely at 2nm. This means that at this concentration, the number of the high aggregates is reduced as compared with those at 2 nm. Both size and the number of the populations increase at higher concentration (1%), as can be seen in Fig. 3b.

The AFM image of the film cast from 0.5% DMF solution on glass substrate reveals the presence of spherical aggregates of the order 1-2  $\mu\text{m}$  (Fig. 4a). Thus, the structuration in solution emphasized by other techniques (surface tension, viscometry, UV-Vis absorption, DLS) is perpetuated in film as was already proved by SEM investigations [11]. The higher aggregate dimensions as compared with those measured by DLS would be explained by the stepwise increasing in solution concentration as the solvent is evaporated. In phase mode analysis, there was no indication for biphasic morphology (Fig. 4b). Average roughness estimated on an 1x1 $\mu\text{m}$  area was  $S_a = 5.16239$  nm.

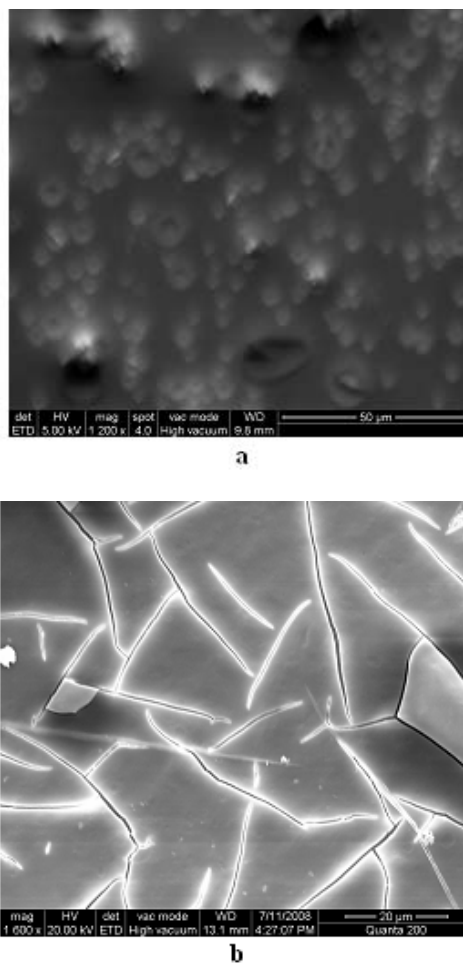


Fig. 5. SEM image of the cast CEN 22 film (a-CEN22C) subsequently IR irradiated (b-CEN22-CIR).

The surface morphology is completely modified by IR irradiation and thermal treatment at 200°C (see Experimental section, sample CEN22-CIR-200). As can be observed in Fig. 4c,d, the granular morphology in the case of CEN22-C changes into a fibrillar one. According to our previously reported DSC and POM investigations, this compound exhibited multiple endothermal transitions below 200°C [12]. So, the annealed films undergo melting and isotropization during the thermal treatment. This can explain the different morphology between the treated and untreated samples based on different models of chain packing as a function of annealing conditions. In the

literature is stated that in such cases  $\pi$ -stacking can occur, thus the fibrillar structure is favored [15].

The changing in the film morphology as a result of the IR irradiation was also emphasized by SEM image (ETD) (Fig. 5).

The results obtained by EDX technique revealed the presence of the domains having different compositions on the film (Fig. 6). Silicon and oxygen seem to be predominant within the fibrillar domains as can be seen in the elemental distribution charts. All expected elements are present on the rest of the surface having a relatively uniform distribution.

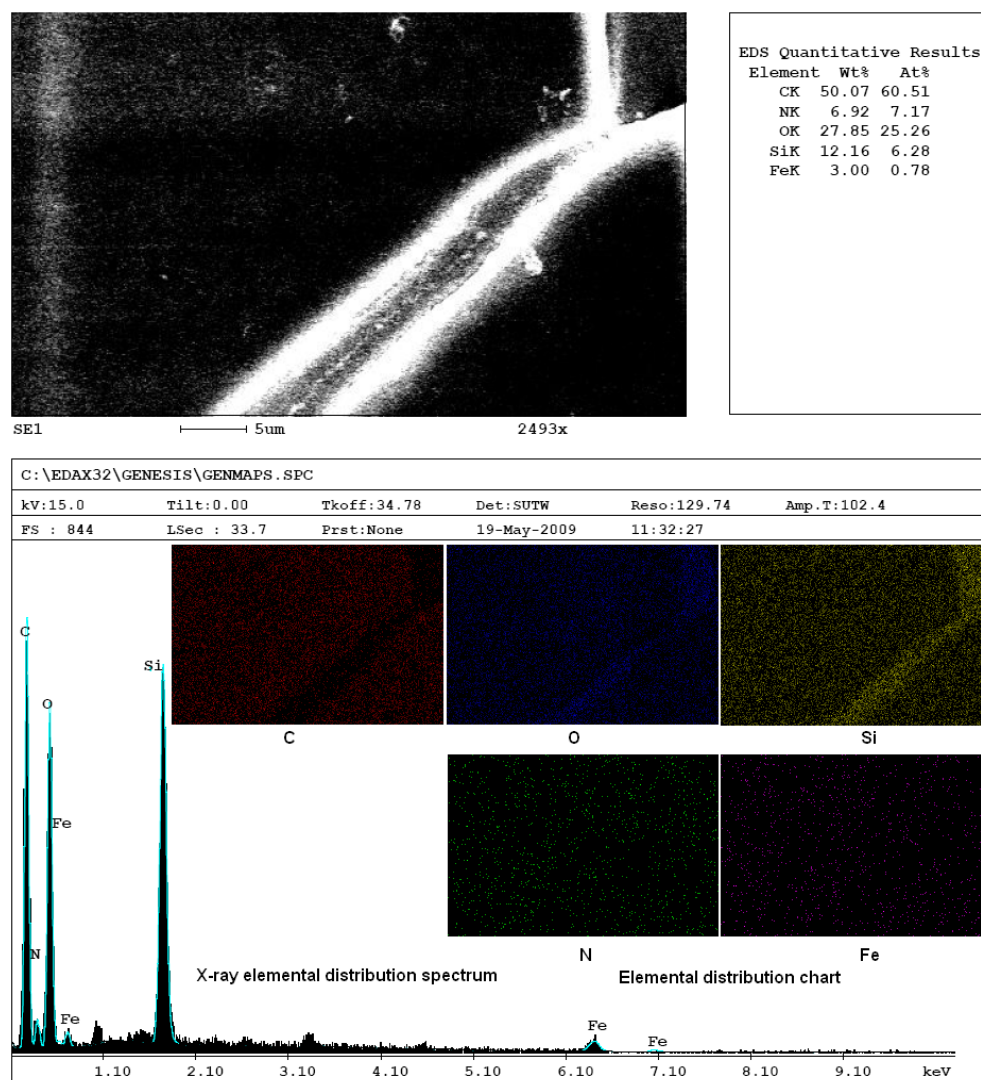


Fig. 6. EDX analysis results for the sample CEN22 processed as film from DMF.

XRD pattern of both CEN22-C and CEN22-SC reveals a stable cvasi-crystalline structure (Fig. 7). The large peak located around  $2\theta = 25$  degree can be deconvoluted in two gaussian ones.

However, it can be noticed the influence of the film treatment procedure on the XRD pattern. Thus, the raw and irradiated CEN22-C cast films show another two

peaks at  $2\theta = 4,8$  (CEN-22C) or 5.6 degree (CEN22-CIR) and  $2\theta = 43$  degree. The presence of diffraction maxima in the low angle region indicates a layered structure typical for smectic liquid crystalline compounds. The calculated interplane distance is 18.3Å (for CEN22C) and 15.7Å (for CEN22CIR). Indeed, the liquid crystalline behavior was emphasized in our previous study [12]. The narrow peak at

$2\theta = 43$  degree showed by the two samples is usually assigned to XRD peak (400) of  $\gamma\text{-Fe}_2\text{O}_3$  phase. It is possible that in the processing conditions (IR) a  $\text{Fe}^{2+} \rightarrow \text{Fe}^{3+}$  oxidation to occur. By annealing at  $200^\circ\text{C}$ , these peaks disappear in all cases (CEN22-C200, CEN22-CIR200, and CEN22-SC200). The same XRD pattern without narrow peaks was obtained for the film prepared by spin coating and annealed at  $200^\circ\text{C}$ . We presume that by thermal treatment at  $200^\circ\text{C}$ , the order is disrupted due to the melting that was detected by Differential Scanning Calorimetry (DSC) [12]. The subsequent cooling either does not permit the order recovering (CEN22-C200) or induces a new recrystallization (CEN22-CIR-200).

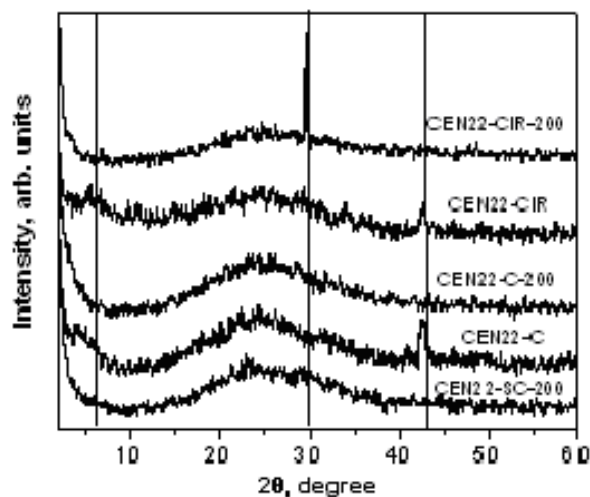


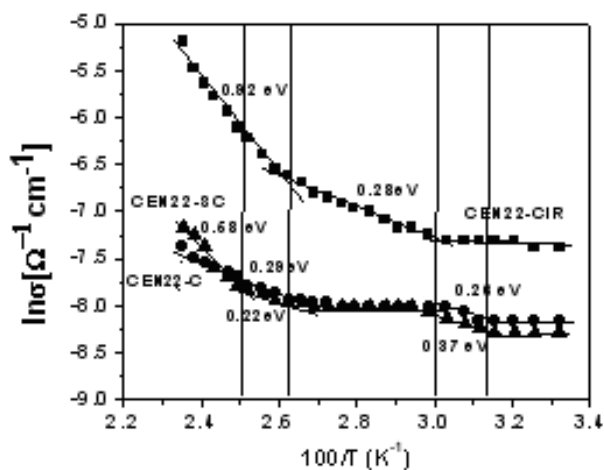
Fig. 7. XRD pattern of thin films

The electrical resistance in air has been measured by the two probes method. The resistance dependence on temperature was studied. The sample was heated in an oven that assures a good thermal contact and permits the well-controlled temperature variation.

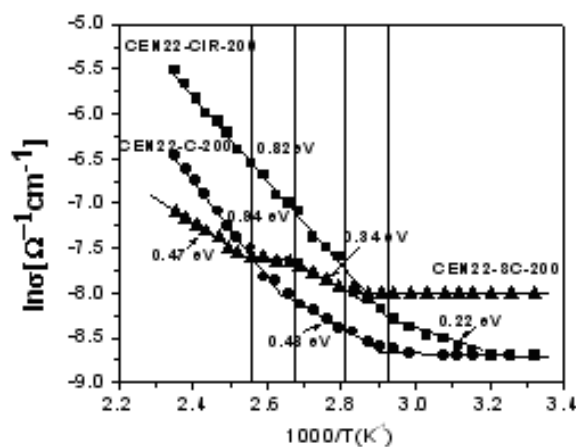
Our previous researches established that, for organic semiconductors, samples with stable structures and reproducible properties can be obtained if these are thermally treated. In general, this consists in successive heating and cooling cycles in certain temperature range specific to every polymer. The stabilization of the polymer's structure is important when the values of some parameters (e.g., activation energy) are determined by the temperature dependence of the transport process coefficients. In this case, during heating, structural modifications can occur that masks the process.

On the studied temperature range (300 K-575 K), the exponential increasing of the electrical conductivity with temperature can be observed (Fig. 7). This dependence is reversible for the thermal treated sample. In general, for

such samples this dependence,  $\ln\sigma=f(10^3/T)$ , shows a region having lower slope in the low temperatures range in which extrinsic conduction can be considered to occur. The hopping conduction model can explain this behavior. In the higher temperatures field ( $T>T_C$ ,  $T_C$  being a temperature specific for every sample) it can be presumed that the polymers possess an intrinsic conduction.



a



b

Fig. 8. Dependence of  $\ln(\sigma) = f(1000/T)$  for films prepared and annealed in different conditions: a-raw films; b-annealed at 473K.

The electrical conductivity slightly increases in the case of the spin coated as compared with cast films, as well as by thermal treatment at  $200^\circ\text{C}$  (Table 1).

Table 1. The main parameters of the electrical measurements

Sample	$\sigma_c \cdot 10^4 (\Omega^{-1} \text{cm}^{-1})$	$\Delta T$ (K)	$\Delta E$ (eV)
CEN22-C	2.85	318 -335	0.26
		376-425	0.29
CEN22-C-200	1.66	340-376	0.48
		376-425	0.94
CEN22-CIR-200	1.66	348-425	0.82
CEN22-SC	6.25	318-385	0.28
		386-425	0.92
CEN22-SC-200	3.33	358-372	0.34
		372-425	0.47

$\sigma_c$  – electrical conductivity at room temperature (300K);  $\Delta E$ - thermal energy for the activation of the electrical conductivity for different  $\Delta T$  temperature ranges.

It is considered that the dependence between electrical conductivity and temperature is described by the relationship:

$$\sigma = \sigma_0 \cdot \exp\left(-\frac{\Delta E}{2kT}\right)$$

where  $\Delta E$  - thermal energy for the activation of the electrical conductivity and  $\sigma_0$  is a parameter depending on the semiconductor nature. The activation energy can be determined from the slope of the function  $\ln \sigma = f(10^3/T)$ .

#### 4. Conclusions

Even though the approached copolymer is segmented one having low molecular weight and short monomer sequences, this proved to possess association ability in solution that is perpetuated in the film. Aggregates having diameter of about 20nm were measured by DLS (Malvern).  $^1\text{H}$  NMR studies in solvents of different polarity and different concentrations and temperatures confirmed the association phenomena. The studies by SEM, AFM, and XRD reveal that the morphology is strongly influenced by the applied annealing procedure. The morphological changes are reflected in the electrical conductivity.

#### Acknowledgments

This research has been financially supported by Project PNCD II-PC (Contract nr. 12-128/1.10.2008). The authors are grateful to Dr. Aurica Chiriac and Dr. Loredana Nita for DLS measurements (Malvern).

#### References

- [1] T. Fahmi Pletsch, C. Mendoza, N. Cheval, *Materials Today* **12**(5), 44 (2009).
- [2] I. Yilgor, J. E. McGrath, *Adv. Polym. Sci.* **86**, 1 (1988).
- [3] X. S. Wang, M. A. Winnik, I. Manners, *Macromolecules* **35**, 9146 (2002).
- [4] R. Resendes, J. A. Massey, H. Dorn, K. N. Power, M. A. Winnik, I. Manners, *Angew. Chem. Int. Ed.* **38**(17), 2570 (1999).
- [5] J. Massey, K. N. Power, I. Manners, M. A. Winnik, *J. Am. Chem. Soc.* **120**, 9533 (1998).
- [6] J. A. Massey, K. Temple, L. Cao, Y. Rharbi, J. Raez, M. A. Winnik, I. Manners, *J. Am. Chem. Soc.* **122**, 11577 (2000).
- [7] R. H. Lammertink, M. A. Hempenius, G. J. Vancso, K. Shin, M. H. Rafailovich, J. Sokolov, *Macromolecules* **34**, 942 (2001).
- [8] R. Resendes, J. A. Massey, K. Temple, L. Cao, K. N. Power-Billard, M. A. Winnik, I. Manners, *Chem. Eur. J.* **7**(11), 2414 (2001).
- [9] A. Shimojima, K. Kuroda, *Chem Rec* **6**, 53 (2006).
- [10] S. Sakurai, *Polymer* **49**, 2781 (2008).
- [11] M. Cazacu, C. Racles, A. Airinei, M. Alexandru, A. Vlad, *J. Polym. Sci. Polym. Chem.* **47**(21), 5845 (2009).
- [12] M. Cazacu, A. Vlad, M. Marcu, C. Racles, A. Airinei, G. Munteanu, *Macromolecules* **39**, 3786 (2006).
- [13] C. M. Casado, M. Moran, J. Losada, I. Cuadrado, *Inorg. Chem.* **34**, 1668 (1995).
- [14] X. Zushun, F. Linxian, J. Jian, C. Shiyuan, C. Yongchun, Y. Changfeng, *Eur. Polym. J.* **34**, 1499 (1998).
- [15] Ph. Leclere, R. Lazzaroni, J. L. Bredas, J. M. Yu, Ph. Dubois, R. Jerome, *Langmuir*, **12**(18), 4317 (1996).

\*Corresponding author: mcazacu@icmpp.ro